Role of Copper in Thermal Stability of Human Ceruloplasmin

Erik Sedlák,* Gabriel Žoldák,† and Pernilla Wittung-Stafshede*‡§

*Department of Biochemistry and Cell Biology, Rice University, Houston, Texas 77251; †Laboratorium für Biochemie, Universität Bayreuth, D-95440 Bayreuth, Germany; ‡Keck Center for Structural Computational Biology, Rice University, Houston, Texas 77251; and §Department of Chemistry, Rice University, Houston, Texas 77251

ABSTRACT Human ceruloplasmin (CP) is a multicopper oxidase essential for normal iron homeostasis. The protein has six domains with one type-1 copper in each of domains 2, 4, and 6; the remaining coppers form a catalytic trinuclear cluster at the interface between domains 1 and 6. To assess the role of the coppers in CP thermal stability, we have probed the thermal unfolding process as a function of scan rate of holo- and apo-forms using several detection methods (circular dichroism, aromatic and 8-anilino-naphthalene-1-sulfonic acid fluorescence, visible absorption, activity, and differential scanning calorimetry). Both species of CP undergo irreversible thermal reactions to denatured states with significant residual structure. For identical scan rates, the thermal midpoint appears at temperatures 15–20° higher for the holo- as compared with the apo- form. The thermal data for both forms were fit by a mechanistic model involving two consecutive, irreversible steps ($N \rightarrow I \rightarrow D$). The holo-intermediate, *I*, has lost one oxidized type-1 copper and secondary structure in at least one domain; however, the trinuclear copper cluster remains intact as it is functional in oxidase activity. The activation parameters obtained from the fits to the thermal transitions were used to assess the kinetic stability of apo- and holo-CP at physiological temperatures (i.e., at 37°C). It emerges that native CP (i.e., with six coppers) is rather unstable and converts to *I* in $<$1 day at 37°C. Nonetheless, this form remains intact for more than 2 weeks and may thus be a biologically relevant state of CP in vivo. In contrast, apo-CP unfolds rapidly: the denatured state is reached in $<$2 days at 37°C.

INTRODUCTION

Ceruloplasmin (CP; EC 1.16.3.1) is a multicopper protein widely distributed in vertebrates. It occurs mainly in the plasma and plays an important role in iron homeostasis (1,2). Other roles include its participation in the antioxidant defense (3–6) or in oxidative damage mechanisms (7,8) and its involvement in a number of processes related to the metabolism of copper (9), biogenic amines (10), and nitric oxide (11).

Human ceruloplasmin is a single chain of 1046 amino acids (12) with a carbohydrate content of 7–8% and six integral copper ions. The x-ray structure has shown that CP is composed of six compact β-barrel domains with large loop insertions and that the six copper ions are distributed in one trinuclear copper cluster (involving type-2 and type-3 copper ions) located at the border between domains 1 and 6 and possessing ligands from each domain, and in three mononuclear type-1, or ''blue'', sites (13). The mononuclear copper sites located in domains 4 and 6 of CP are typical type-1 sites, like that in ascorbate oxidase (14), and have four ligands (two histidines, one cysteine, and one methionine) arranged in a distorted tetrahedral geometry. The type-1 copper site located in domain 2 is instead a tricoordinated type-1 site in that it lacks an axial Met ligand. This position is replaced by Leu in CP, like blue-copper sites in some laccases (15), and in Fet3 (16). The type-1 copper in domain 2 has been found to be permanently reduced and is not involved in catalytic activity (17,18). CP is synthesized in hepatocytes and secreted into the plasma after incorporation of six copper ions in the secretory pathway (19). Failure to incorporate copper during biosynthesis results in the secretion of an unstable polypeptide that is rapidly degraded in the plasma (20). In Wilson's disease, the absence or impaired function of a copper-transporting ATPase disrupts copper translocations into the secretary pathway, resulting in decreased serum levels of CP in affected patients (21). Aceruloplasminemia, an autosomal recessive neurodegenerative disease, is associated with mutations in the CP gene and accompanied by absence of CP oxidase activity (22).

Previous studies have indicated that the conformation of apo-CP is different from that of the holoprotein (23,24). It was proposed that the apo- form has molten-globule-like properties, although a significant amount of residual tertiary structure remained (23). For more than 40 years, the working model has assumed that CP binds copper in an all-or-none fashion (25). In support, recent metabolic labeling experiments indicated that achieving the final state of CP required occupation of all six copper-binding sites, with no apparent hierarchy for incorporation at any given site (19). On the other hand, there have also been a number of reports that invoke the possibility of partially metalated forms of CP (26,27). Based on cyanide-dependent metal-removal attempts, it was suggested that the type-1 coppers are more sensitive than the type-2 and type-3 coppers to elimination (27,28). Very recently, we showed that chemically induced equilibrium denaturation of CP at room temperature proceeds through an intermediate (*I*) that has lost two copper ions (29). Whereas the *I* forms reversibly, complete unfolding and loss of all copper ions result in an irreversibly

Submitted May 29, 2007, and accepted for publication October 3, 2007.

Address reprint requests to P. Wittung-Stafshede, Tel.: 713-348-4076; Fax: 713-348-5154; E-mail: pernilla@rice.edu.

The permanent address for Erik Sedlák and Gabriel Žoldák is Dept. of Biochemistry, P. J. Safarik University, Moyzesova 11, 04001 Kosice, Slovakia.

Editor: Jonathan B. Chaires.

0006-3495/08/02/1384/08 $2.00

doi: 10.1529/biophysj.107.113696

denatured state. Attempts to refold this species at pH 7 result in the formation of a misfolded molten globule, regardless of the presence or absence of copper ions (29).

To analyze the role of copper in thermal stability, we have investigated the thermal denaturation reactions of holo- and apo- forms of human CP by circular dichroism (CD), fluorescence, visible absorption, oxidase activity, and differential scanning calorimetry (DSC) methods. The thermal reactions were analyzed according to Lyubarev and Kurganov's model (30) for two consecutive irreversible steps. The data reveal the presence of a partially folded intermediate, with (for the holo- form) an intact trinuclear site but loss of one or two type-I coppers at intermediate temperatures. The activation parameters extracted from fits to thermal transitions at different scan rates were used to predict the kinetic behavior of CP at 37°C (pH 7). It emerges that the native, six-copper form of CP is rather unstable at this temperature (half-life of 14 h), whereas the intermediate form remains intact for weeks; the latter species may therefore be present during in vivo CP circulation.

EXPERIMENTAL PROCEDURES

Chemicals and instruments

Analytical-grade chemicals and *o*-dianisidine were obtained from Sigma-Aldrich (St. Louis, MO). 2,2′- Biquinoline was obtained from Fluka (Seelze, Germany). Human CP (>95% purity, $A_{610}/A_{280} = 0.046$) was obtained from Vital Products (Boynton Beach, FL). Concentration of holo- and apo-CP was determined by ε_{280nm} of 200 $mM^{-1}cm^{-1}$. Absorbance and far-UV CD measurements were performed on Varian Cary 50 and Jasco J-810 spectrometers, respectively.

Copper removal

To prepare apo-CP, 5 mg/ml of CP was dialyzed for 2 h at 4°C against 50 mM ascorbate in 0.1 M TrisHCl, pH 7.2. Subsequently, dialysis continued for 12–14 h at 4°C against 50 mM NaCN, 10 mM EDTA, and 10 mM ascorbate in 0.1 M TrisHCl, pH 7.2. The dialysis proceeded for another 16 h at 4°C (with buffer exchange after 8 h) against 50 mM sodium phosphate buffer, pH 7.0. The final apo- form of CP prepared this way contained 0.6 ± 0.4 coppers/CP, as determined by the method developed by Felsenfeld (31).

Activity assay

Oxidase activity of CP was tested using *o*-dianisidine as a substrate in accordance with the procedure by Schosinsky et al. (32). CP activity as a function of temperature was determined as follows: a sample with CP was heated at a rate of 1 K/min; after the desired temperature was reached, a 25-μl aliquot of CP solution was transferred into 100 μl 100 mM acetate, pH 5.0, and cooled on ice. The activity was measured at 23°C.

DSC

DSC experiments were performed on a VP-DSC differential scanning microcalorimeter (Microcal, Northampton, MA) at scan rate of 1.0 K/min. Protein concentration was 3–4 μM (pH 7). Before measurements, sample and reference solutions were properly degassed in an evacuated chamber for 5 min at room temperature and carefully loaded into the cells to avoid bubble formation. Exhaustive cleaning of the cells was undertaken before each experiment. A pressure of 2 atm was kept in the cells throughout the heating cycles to prevent degassing. A background scan collected with buffer in both cells was subtracted from each scan. The reversibility of the transitions was assessed by the reproducibility of the calorimetric trace in a second heating cycle performed immediately after cooling from the first scan. Excess heat capacity curves were plotted using Origin software supplied by Microcal.

CD

CD spectra in the far-UV range (190–250 nm) were recorded on a Jasco-810 instrument with cell path of 1 mm and protein concentrations of 0.3–0.4 μM. Each spectrum is an average of 10 scans. All spectra were background-corrected and converted to mean residue ellipticity (deg·cm^2/dmol). The thermal CD experiments were monitored at 210 nm using a constant heating rate of 0.5, 1, or 1.5 K/min in separate experiments.

Fluorescence

Samples of the holo- or apo- form (~3 μM) of CP were mixed with 200 μM 8-anilino-naphthalene-1-sulfonic acid (ANS) and incubated for 1 h at 23°C. The sample temperature was increased at a constant scan rate (0.5, 1, or 1.5 K/min in separate experiments). The same sample was monitored both for tryptophan and ANS fluorescence at 335 nm (excitation at 295 nm) and 510 nm (excitation at 390 nm), respectively.

Data analysis

DSC-, fluorescence-, and CD-monitored thermal transitions were analyzed according to the model by Lyubarev and Kurganov involving two consecutive irreversible steps of reaction:

$$N \xrightarrow{k_1} I \xrightarrow{k_2} D, \tag{1}$$

where N, I, and D are native, partially denatured, and denatured states, respectively, and k_1 and k_2 are rate constants of corresponding reactions (30). This model is described by a set of differential equations (see Results). Differential equations were solved numerically, and the sum of squared differences between experimental and generated points was minimized. Standard deviations were calculated using 10 sets of the generated data with added Gaussian white noise. Distribution moments of the noise were modeled according to the resulting distribution of the residuals. The correlation coefficient (R) was calculated as:

$$R = \sqrt{1 - \sum_{i=1}^{n}(y_i - y_i^{calc})^2 / \sum_{i=1}^{n}(y_i - y_i^{m})^2}, \tag{2}$$

where y_i and y_i^{calc} are, respectively, the experimental and calculated values of C_p^{ex}; y_i^m is the mean of the experimental values of C_p^{ex} and n is the number of points (e.g., (33)).

Time dependence of the mole fractions γ_N, γ_I, and γ_D of the three different forms of CP (N, I, and D) at 37°C were obtained from the following analytical equations:

$$\gamma_N = \exp(-k_1 t) \tag{3}$$

$$\gamma_I = \frac{k_1}{k_2 - k_1}[\exp(-k_1 t) - \exp(-k_2 t)] \tag{4}$$

$$\gamma_D = 1 + \frac{1}{k_1 - k_2}[k_2 \exp(-k_1 t) - k_1 \exp(-k_2 t)], \tag{5}$$

where the rate constants at any given temperature can be obtained from the Arrhenius equation, $k = A\exp(-E_a/RT)$, where A is the preexponential factor, E_a is the energy of activation, and R is the gas constant. It is convenient to use an alternative form of the Arrhenius equation where the parameter

T^* (temperature at which rate constant equals 1 min^{-1}) is used instead of the parameter A:

$$k = \exp[E_a/R(1/T^* - 1/T)]. \quad (6)$$

RESULTS

Thermal denaturation of CP monitored by far-UV CD

Thermal denaturation of holo- (i.e., six copper) and apo- (i.e., no copper) forms of CP was first monitored by far-UV CD. These experiments show that 1), the thermal transitions of both apo- and holo- forms of CP are irreversible, and 2), they proceed to a state characterized by significant negative ellipticity in the 200- to 210-nm range (Fig. 1). The latter finding indicates that there is residual structure in the thermally denatured state of both apo- and holo-forms. In contrast, chemically denatured CP (at 20°C) has much less negative ellipticity (29), and the far-UV CD spectrum instead matches that of an unfolded protein (Fig. 1). The irreversibility of the thermal transition is not caused by protein aggregation because no signs of aggregation or precipitation were observed. The thermal denaturation processes for both holo- and apo- forms of CP depend on the heating rate: the faster the rate, the higher the apparent thermal midpoint (Fig. 2). Comparing thermal curves at identical scan rates (three different scan rates tested) reveals that the holo- form of CP is more resistant to thermal perturbation than the apo-form by ~15–20°C.

Thermal denaturation of CP monitored by DSC

To obtain more insight into thermal denaturation of CP we next turned to DSC experiments. In Fig. 2, we show DSC data as a function of temperature for both forms of CP at three different scan rates. We note that the transitions observed by CD and DSC at the same scan rate correspond well with each other. The DSC scans clearly demonstrate that the thermal transitions for both forms include at least two steps. From various cooling experiments, we found (as in the CD experiments) that both transitions appear irreversible under our conditions.

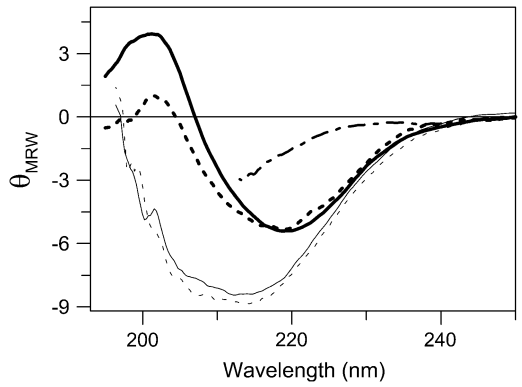

FIGURE 1 CD spectra of N (*thick lines*, at 20°C, pH 7.0) and D (*thin line*, at 70°C, pH 7.0) forms of holo-CP (*solid lines*) and apo-CP (*dotted lines*). For comparison, GuHCl-perturbed CP (at 20°C, pH 7.0) is also shown (*dash-dot line*). CD spectra of 3Cu-CP N and D forms are indistinguishable of those of holo-CP.

Two consecutive irreversible transitions can be described by Eq. 1 in Materials section: $N \xrightarrow{k_1} I \xrightarrow{k_2} D$. This model can be considered a particular case of the Lumry-Eyring model in which the rate of the reverse reaction of the first step is much slower than the rate of the second step (34). Analysis of DSC data using the model of two consecutive irreversible steps has been described in detail by Lyubarev and Kurganov (30). Briefly, the kinetic behavior of the system is described by the following differential equations:

$$\frac{d\gamma_N}{dt} = -k_1\gamma_N \quad (7a)$$

$$\frac{d\gamma_I}{dt} = k_1\gamma_N - k_2\gamma_I \quad (7b)$$

where γ_N and γ_I are the mole fractions of native and partially unfolded protein, respectively. After substituting $dt = dT/\nu$, where ν is the scan rate, and solving the equations, the following is obtained:

$$\gamma_N = \exp\left(-\frac{1}{\nu}\int_{T_0}^{T} k_1 dT\right). \quad (8)$$

$$\gamma_I = \frac{1}{\nu}\exp\left(-\frac{1}{\nu}\int_{T_0}^{T} k_2 dT\right)\int_{T_0}^{T}\left[k_1\exp\left(\frac{1}{\nu}\int_{T_0}^{T}(k_2 - k_1)dT\right)\right]dT. \quad (9)$$

The excess heat capacity, which is the parameter measured in the DSC experiments, is then expressed by the equation:

$$C_p^{ex} = \frac{d\langle\Delta H\rangle}{dT} = \frac{\Delta H_1 k_1}{\nu}\gamma_N + \frac{\Delta H_2 k_2}{\nu}\gamma_I, \quad (10)$$

where ΔH_1 and ΔH_2 are molar enthalpy changes for the first and second steps, respectively. The rate constants, k, are related to E_a and T^* via Eq. 6. The DSC data in Fig. 2 were fitted to Eq. 10, and the resulting six parameters (ΔH_1, ΔH_2, E_{a1}, E_{a2}, T_1^*, and T_2^*) are listed in Table 1.

In analogy, the temperature dependences of the CD and fluorescence signals were fitted by the following equation:

$$S_{obs} = S_N\gamma_N + S_I\gamma_I + S_D(1 - \gamma_N - \gamma_I), \quad (11)$$

where S_{obs}, S_N, S_I, and S_D are measured signal and signals of native, partially denatured, and denatured states, respectively. In combination with the expressions for each mole fraction given in the equations above (using CD signals instead of enthalpy changes), and the relation among k, E_a, and T^* provided by Eq. 6, the key parameters (i.e., E_a and T^* values) could be obtained from fits to the CD-detected profiles (Table 1). The parameters for the first transition (N to I) obtained from CD differ somewhat from those obtained from DSC. This is likely an effect of the poor separation of the two thermal steps when probed by CD, causing unreliable fits. The theoretical

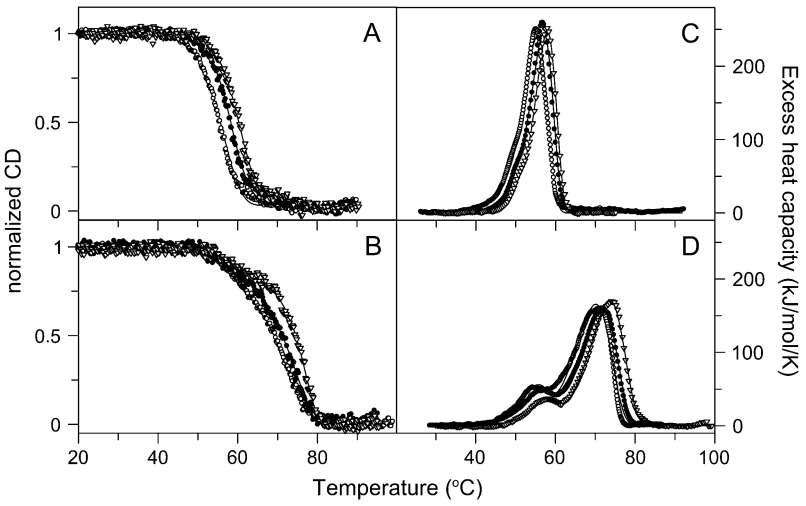

FIGURE 2 Thermal transitions of apo- (*A* and *C*) and holo- (*B* and *D*) forms of CP monitored by CD and DSC. Ellipticity dependence monitored at 210 nm is shown as normalized ellipticity. Measurements were performed at three different scan rates (from *left*: 0.5, 1.0, and 1.5 K/min) at pH 7.0. DSC scans were performed at three different scan rates (from *left*: 0.5, 1.0, and 1.5 K/min) at pH 7.0. Experimental data are shown as points; theoretical fits based on Eqs. 10 and 11 are shown as solid lines.

DSC and CD curves based on the fitted parameters are shown in Fig. 2 and are in good agreement with the actual data. This supports the two-step irreversible mechanism as an appropriate assumption.

Thermal denaturation of CP monitored by other methods

To further investigate the thermal reactions of CP, tryptophan fluorescence and fluorescence of ANS were probed as a function of temperature. CP has 19 tryptophans that are scattered throughout the six domains. Normalized tryptophan and ANS fluorescence signals of apo- and holo- forms of CP as a function of temperature are shown in Fig. 3 for three different scan rates. Whereas the data for apo-CP adopt an asymmetrical sigmoidal shape (Fig. 3 *A*), holo-CP fluorescence data clearly show three-state behavior (Fig. 3 *B*). For both holo- and apo-forms, the tryptophan-emission changes as a function of temperature were not affected by the presence or absence of ANS. Thus, ANS in itself did not have any effect on CP thermal

TABLE 1 Calculated parameters based on two-step analysis of the data shown in Figs. 2 and 3 describing the irreversible thermal transitions of holo- and apo- forms of human CP

CP form	E_{a1} (kJ/mol)	T^*_1 (K)	ΔH_1 (kJ/mol)	E_{a2} (kJ/mol)	T^*_2 (K)	ΔH_2 (kJ/mol)	R	T_{obs}† (°C)
Apo								**1st/2nd**
DSC 0.5 K/min	222	332	407	275	334	1571	0.9980	50.9/55.5
DSC 1.0 K/min	273	328	365	326	333	1593	0.9975	52.7/57.0
DSC 1.5 K/min	267	330	394	323	333	1401	0.9994	53.9/58.0
Average	254	330	389	308	333	1521		
F_{Trp} 0.5 K/min	238	334	–	240	334	–	0.9999	54.1
F_{Trp} 1.0 K/min	274	334	–	331	335	–	0.9997	55.6
F_{Trp} 1.5 K/min	239	334	–	322	331	–	0.9999	56.6
CD 0.5 K/min	181	341	–	176	335	–	0.9991	55.3
CD 1.0 K/min	167	341	–	298	332	–	0.9985	57.9
CD 1.5 K/min	187	340	–	265	332	–	0.9979	59.9
Holo								
DSC 0.5 K/min	268	334	420	219	353	1917	0.9934	55.0/71.6
DSC 1.0 K/min	219	335	443	230	351	1801	0.9989	56.5/72.4
DSC 1.5 K/min	275	333	381	232	351	1930	0.9990	57.4/74.0
Average	254	334	415	227	351	1883		
F_{Trp} 0.5 K/min	275	334	–	175	358	–	0.9996	54.1/70.0
F_{Trp} 1.0 K/min	278	333	–	213	354	–	0.9998	56.4/72.6
F_{Trp} 1.5 K/min	232	336	–	221	355	–	0.9998	58.5/75.9
CD 0.5 K/min	174	347	–	210	357	–	0.9995	56.7/71.1
CD 1.0 K/min	152	348	–	235	354	–	0.9986	59.0/73.1
CD 1.5 K/min	118	354	–	337	352	–	0.9987	61.6/75.0

T^* values are the temperatures at which the rate constant for the specific reaction is 1/min. Index 1 corresponds to the first *N*-to-*I* transition, and index 2 corresponds to the subsequent *I*-to-*D* process. The DSC data are most reliable and were used to derive average values for each parameter. R is the correlation coefficient (see Eq. 4).

†Observed thermal midpoints; for some apo-CP data, only the midpoint of the major transition is reported.

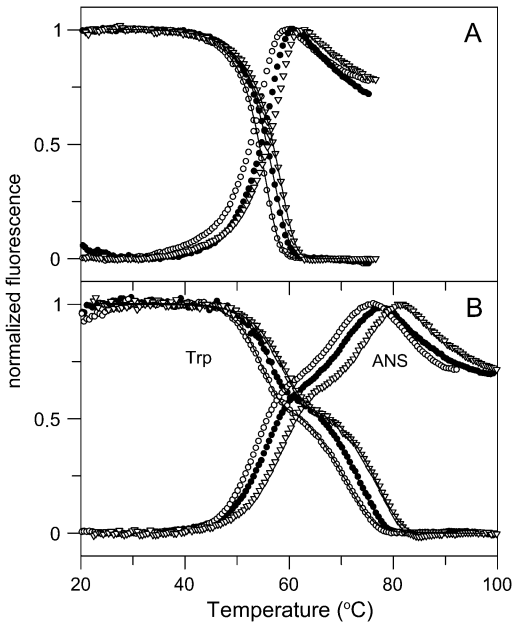

FIGURE 3 Thermal transitions of apo- (*A*) and holo- (*B*) forms of CP monitored by tryptophan fluorescence (emission wavelength 335 nm) and ANS fluorescence (emission wavelength 510 nm). Fluorescence is shown as normalized ellipticity. Measurements were performed at three different scan rates (from *left*: 0.5, 1.0, and 1.5 K/min) at pH 7.0. Experimental data are shown as points; theoretical fits based on Eq. 11 are shown as solid lines.

stability. The obtained parameters from fits to the tryptophan fluorescence, again assuming a two-step, irreversible reaction mechanism, are in good agreement with the parameters obtained from the DSC data (Table 1). The ANS emission increases on CP denaturation, with the *I* species having an intermediate-sized signal. This implies that *I* is not a partially folded molten-globule-like species, as such structures tend to bind ANS strongly, causing orders of magnitude higher ANS emission. (The ANS emission data were not analyzed further because of the nonlinearity of the posttransition regions.)

For holo-CP, 610-nm absorbance was also investigated as a function of temperature (Fig. 4). Absorbance at 610 nm monitors the two oxidized type-1 copper sites in CP, i.e., the coppers in domains 4 and 6. The high reduction potential of

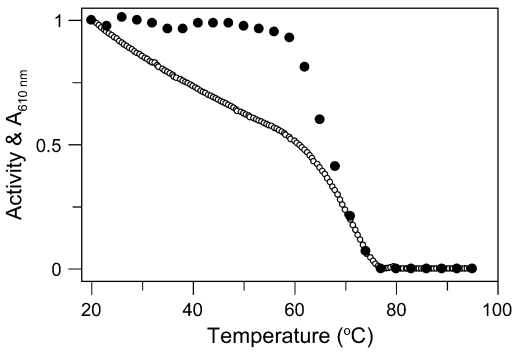

FIGURE 4 Thermal dependence of absorbance of holo-CP at 610 nm (○) and oxidase activity at 20°C (●) after heating to the indicated temperatures.

the type-1 copper in domain 2 has indicated that it is permanently reduced; thus, it does not contribute to the blue color, nor is it catalytically relevant (17,18). We find that 610-nm absorption of holo-CP decreases gradually with temperature up to ~60°C, where it adopts a signal that is ~50% of its original value at 20°C. At higher temperatures, the remaining visible absorption rapidly decreases toward zero. This result indicates perturbation (and likely metal dissociation) of the two type-1 copper sites in two phases as a function of temperature; one copper goes in the first step, the other in the second step. The first phase correlates with the formation of the *N*-to-*I* step as detected by CD, fluorescence, and DSC; the second phase correlates with the *I*-to-*D* step detected by the other methods.

Also CP's oxidase activity parameters were obtained as a function of temperature (Fig. 4). Aromatic diamine (*o*-dianisidine) oxidation by CP requires an intact trinuclear copper site, which is situated on the interface between domains 1 and 6. The type-1 copper site in domain 4 is likely the entry point of the electrons from this substrate before transfer to the catalytic cluster (10). When CP solutions heated to different temperatures were cooled to 23°C and oxidase activity was measured, native-like activity was found for samples heated to temperatures up to 60°C. This indicates that the structural changes of the first phase (*N* to *I*) include distortion of parts of the protein not involved in catalytic activity. Further increase in temperature leads to irreversible inhibition of CP oxidase activity with an apparent transition midpoint at 68°C. This process correlates with the second step (i.e., *I* to *D*) observed by DSC and the spectral methods. Based on these results, we conclude that the trinuclear site is destroyed in the *I*-to-*D* step.

DISCUSSION

Human CP is a key protein in copper/iron metabolism (35,36). It is linked to diseases such as aceruloplasminemia and Wilson's disease. From a biophysical point, it is an intriguing, complex protein with six integral coppers distributed in a structure of six β-sandwich domains. We recently reported chemical unfolding data on apo- and holo- forms of human CP. We found that urea-induced unfolding involves an intermediate with loss of about two type-1 coppers (one being the permanently reduced one in domain 2). Complete unfolding was irreversible because attempts to refold from this starting point resulted in a dead-end molten globule species (29). Less is known about CP thermal unfolding. Thermal denaturation of sheep CP was reported to be irreversible and to have a T_{trs} of >70°C (37). However, for irreversible reactions, a high melting temperature does not guarantee that a protein will remain in its native state for a given time at a certain temperature (38). In such cases, information about the structural integrity of proteins can only be obtained from kinetic parameters. The physical basis of protein kinetic stability is, however, poorly understood, and no structural consensus has been found to explain this phenomenon (39).

In this study, we assessed the thermal reaction of human CP in its apo- and copper-loaded forms to reveal details about kinetic stability and specific roles of the coppers. Previously, copper has been found to add to both equilibrium and kinetic stability of some proteins (i.e., azurin, ascorbate oxidase, Cu, Zn-superoxide dismutase) (40–44). However, it has also been shown that copper can decrease the stability of proteins. For example, copper ions 1), promote transitions in the prion protein toward less thermally stable conformations (45), 2), limit the reversibility of thermal transitions of blue-copper proteins (46–48), and 3), bind specifically to nonnative states of β_2-microglobulin, resulting in a destabilization of the native state (49). Our work presented here reveals that in the case of human CP, the protein is thermally and kinetically stabilized by its copper cofactors.

We have found that the thermal reaction of CP (both apo- and holo- forms) is irreversible and involves two phases. An irreversible two-step model was therefore used to analyze thermal data collected by a set of different detection methods (i.e., CD, fluorescence, and DSC). The similar parameters derived from data collected by the different detection methods, and for data collected with different scan rates, strongly support the validity of the assumed denaturation mechanism. Based on the spectroscopic data (Fig. 2), the holo-intermediate species has slightly perturbed secondary structure and exposes 50–70% of its tryptophans to the solvent (Fig. 3). The enthalpy data (Table 1) suggest that formation of the intermediate corresponds to about one-sixth of the overall enthalpy change associated with the overall reaction (ΔH_1 is about one-sixth of total enthalpy change for holo-CP). These numbers suggest that the intermediate has one or two domains (of the six) unfolded. Because there is no significant increase in ANS emission at the conditions favoring the thermal intermediate, a partially folded species is disfavored over a species with most domains fully folded and a few (or one) domains fully unfolded.

The blue color experiments (Fig. 4) indicate that the holo-intermediate has lost one oxidized type-1 copper, and the activity experiments imply that the trinuclear cluster is intact in the intermediate species. The oxidized type-1 copper that is removed in the intermediate could be the one in either domain 4 or 6. We propose that it is more likely that it is the one in domain 4, as disruption of the type-1 site in domain 6 (for example, through domain unfolding) would likely also perturb the interface between domains 6 and 1 and therefore affect the trinuclear copper site. It is also possible that the copper loss in the first unfolding step corresponds to a small disruption of the metal site and that the affected protein domain (i.e., domain 4 or 6) remains folded. In analogy with the urea-induced holo-CP intermediate observed at room temperature that had lost two coppers (one oxidized and one reduced) (29), we suggest that the reduced type-1 copper in domain 2 is also absent in the thermal holointermediate of CP. We propose that domain 2 is an unfolded domain in the intermediate; if so, the parts of CP involved in oxidase activity are not affected (which is in agreement with our observations) (Fig. 4).

The transition $I \rightarrow D$ is most likely accompanied by structural perturbation in all domains and loss of the trinuclear copper cluster. Based on its CD spectrum, the final thermal state, D, corresponds to a molten-globule species for both apo- and holo-CP (Fig. 1). This species appears similar to the dead-end molten globule detected on refolding attempts in urea from the completely unfolded states of apo- and holo-CP at room temperature (29). The starting state of apo-CP has an open structure and no interactions between domains 1 and 6 (28). Because the $N \rightarrow I$ transition for apo-CP involves a similarly low ΔH_1 as in the case of holo-CP, it is likely that the same domain is perturbed as in the holointermediate. In Fig. 5, a tentative scheme for thermal perturbations of holo- and apo-forms of CP that is based on our data is shown.

Inspection of the parameters from the fits (Table 1) reveals that although the first transition (N to I) is only somewhat stabilized in the holo- form (T_1* increases by 4°), the second step (I to D) is much stabilized in the holo- form (T_2* increases by 18°) as compared with the apo-form data. This implies that although the trinuclear copper cluster (and thus the interactions between domains 1 and 6) contributes to the thermal stability of holo-CP, the type-1 coppers have almost no such effect.

The activation/rate parameters obtained from the fits to the DSC data enabled us to predict the time dependences of the populations of γ_N, γ_I, and γ_D at 37°C (and any other temperature) for apo- and holo- forms of CP via Eq. 5 (Fig. 6). We find that the native state of holo-CP is relatively unstable at

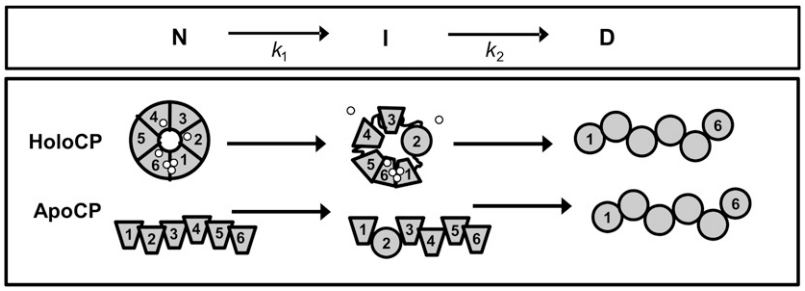

FIGURE 5 Tentative scheme for thermal unfolding of holo- and apo- forms of CP based on our work (*trapezoid* indicates intact domain, and *circle* molten-globule-like domain). We propose that the first *N*-to-*I* transition involves unfolding of one or two domains, perhaps domain 2 as shown here. For holo-CP, the *N*-to-*I* step also couples to type-I copper release. One oxidized type-1 copper is lost (the one in domain 4 is shown, but it could also be the one in domain 6). If domain 2 is unfolded in *I*, it appears reasonable that the reduced type-1 copper in this domain is also lost (as shown here). This was previously concluded to be the case for the urea-induced CP intermediate (29). The last step involves destruction of the trinuclear copper cluster and structural perturbations in all domains.

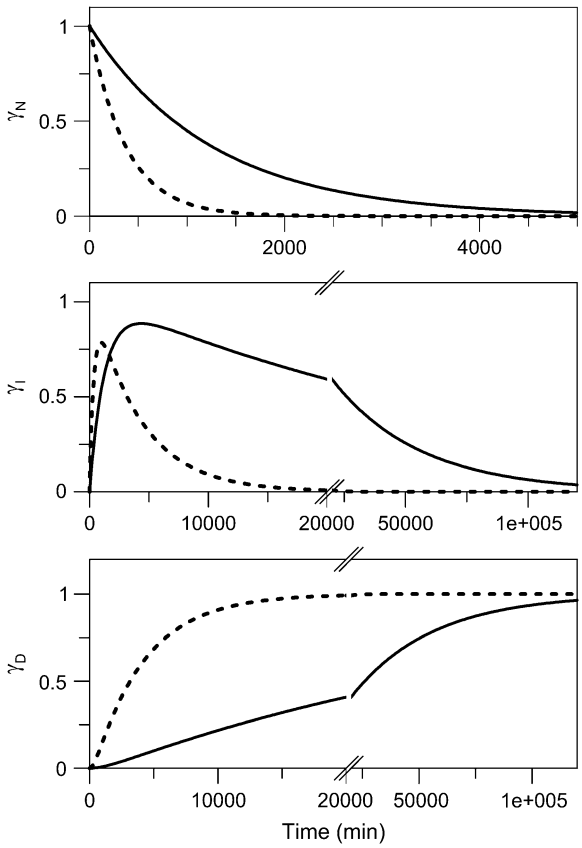

FIGURE 6 Time dependence of mole fractions γ_N, γ_I, and γ_D of holo- (*solid lines*), and apo- (*dotted lines*) forms of CP at 37°C. The kinetics were obtained from Eq. 5 using the average parameters from DSC experiments; i.e., for the holo- form ($E_{a,1} = 254$ kJ/mol, $T_1^* = 334$ K, $E_{a,2} = 227$ kJ/mol, $T_2^* = 352$ K): $k_1 = 8.0 \times 10^{-4}$ min^{-1}, and $k_2 = 2.8 \times 10^{-5}$ min^{-1}; and for the apo- form ($E_{a,1} = 254$ kJ/mol, $T_1^* = 330$ K, $E_{a,2} = 308$ kJ/mol, $T_2^* = 333$ K): $k_1 = 2.7 \times 10^{-3}$ min^{-1}, and $k_2 = 2.5 \times 10^{-4}$ min^{-1}, respectively.

physiological temperatures (i.e., 37°C): it transforms to the *I* state with a half-time of ~13.8 h at this temperature. The *I* form of holo-CP is more kinetically stable: its half-life is ~17 days, pH 7, 37°C. Because the ($N \rightarrow I$) conversion occurs on a biologically relevant time scale (i.e., hours at 37°C), both *N* and *I* forms of holo-CP may be present in vivo depending on conditions and copper levels. Removal of copper results in an apoprotein that has less kinetic stability at 37°C. The rate of disappearance of ''native'' apo-CP corresponds to a half-life of 4.3 h (threefold faster than holo-CP). The intermediate species of apo-CP disappears in 1.9 days (i.e., ninefold faster than the holo- form). Notably, direct kinetic unfolding experiments measured by fluorescence of apo- and holo-CP on jumping to different final temperatures (between 42°C and 60°C) matched the values of k_1 and k_2 predicted from the DSC parameters at each temperature (Supplementary Material). This agreement between physical measurements and predictions supports the conclusion that the assumed two-step mechanism is appropriate and thus that the predicted kinetic parameters at 37°C are valid.

CONCLUSIONS

In summary, we show that despite an apparent high thermal stability (observed midpoint at 70–75°C depending on conditions), holo-CP with six intact coppers is a kinetically unstable protein at physiological temperatures (i.e., at 37°C, pH 7). Within hours at this temperature, it converts to a much more inert intermediate species that has lost one or two of the type-1 copper ions. We propose that this intermediate may be present in vivo under some conditions. Our earlier urea experiments (pH 7, 20°C) revealed a similar holo-*I* species that formed reversibly on minor perturbations of the six-copper, fully loaded state of CP (29). In the absence of all coppers, CP is even more unstable; apo-CP is completely unfolded in <2 days at 37°C. The low kinetic stability of the apo- form of CP may correlate with its rapid degradation in vivo in various disease conditions (36).

SUPPLEMENTARY MATERIAL

To view all of the supplemental files associated with this article, visit www.biophysj.org.

This work was funded by grants from the Robert A. Welch Foundation (C-1588) and the US Army Medical Research Acquisition Activity (Concept award W81XWH-06-1-0572).

REFERENCES

1. Frieden, E., and H. S. Hsieh. 1976. Ceruloplasmin: the copper transport protein with essential oxidase activity. *Adv. Enzymol. Relat. Areas Mol. Biol.* 44:187–236.
2. Gitlin, J. D. 1998. Aceruloplasminemia. *Pediatr. Res.* 44:271–276.
3. Gutteridge, J. M. C. 1983. Antioxidant properties of caeruloplasmin towards iron- and copper-dependent oxygen radical formation. *FEBS Lett.* 157:37–40.
4. Miyajima, H., Y. Takahashi, M. Serizawa, E. Kaneko, and J. D. Gitlin. 1996. Increased plasma lipid peroxidation in patients with aceruloplasminemia. *Free Radic. Biol. Med.* 20:757–760.
5. Cha, M. K., and I. H. Kim. 1999. Ceruloplasmin has a distinct active site for the catalyzing glutathione-dependent reduction of alkyl hydroperoxide. *Biochemistry.* 38:12104–12110.
6. Inoue, K., T. Akaike, Y. Miyamoto, T. Okamoto, T. Sawa, M. Otagiri, S. Suzuki, T. Yoshimura, and H. Maeda. 1999. Nitrosothiol formation catalyzed by ceruloplasmin. Implication for cytoprotective mechanism in vivo. *J. Biol. Chem.* 274:27069–27075.
7. Swain, J., and J. M. C. Gutteridge. 1995. Prooxidant iron and copper, with ferroxidase and xanthine oxidase activities in human atherosclerotic material. *FEBS Lett.* 368:513–515.
8. Mukhopadhyay, C. K., B. Mazumder, P. F. Lindley, and P. L. Fox. 1997. Identification of the prooxidant site of human ceruloplasmin: a model for oxidative damage by copper bound to protein surfaces. *Proc. Natl. Acad. Sci. USA.* 94:11546–11551.
9. Harris, E. D. 1993. The transport of copper. *Prog. Clin. Biol. Res.* 380: 163–179.
10. Zaitsev, V. N., I. Zaitseva, M. Papiz, and P. F. Lindley. 1999. An x-ray crystallographic study of the binding sites of the azide inhibitor and organic substrates to ceruloplasmin, a multi-copper oxidase in the plasma. *J. Biol. Inorg. Chem.* 4:579–587.
11. Bianchini, A., G. Musci, and L. Calabrese. 1999. Inhibition of endothelial nitric-oxide synthase by ceruloplasmin. *J. Biol. Chem.* 274:20265–20270.

12. Ortel, T. L., N. Takahashi, and F. W. Putnam. 1984. Structural model of human ceruloplasmin based on internal triplication, hydrophilic/hydrophobic character, and secondary structure of domains. *Proc. Natl. Acad. Sci. USA.* 81:4761–4765.

13. Zaitseva, I., V. Zaitsev, G. Card, K. Moshkov, B. Bax, A. Ralph, and P. Lindley. 1996. The x-ray structure of human serum ceruloplasmin at 3.1 Å: nature of the copper centres. *J. Biol. Inorg. Chem.* 1:15–23.

14. Messerschmidt, A., R. Ladenstein, R. Huber, M. Bolognesi, L. Avigliano, R. Petruzzelli, A. Rossi, and A. Finazzi-Agro. 1992. Refined crystal structure of ascorbate oxidase at 1.9 A resolution. *J. Mol. Biol.* 224:179–205.

15. Solomon, E. I., U. M. Sundaram, and T. E. Machonkin. 1996. Multicopper oxidases and oxygenases. *Chem. Rev.* 96:2563–2606.

16. Hassett, R. F., D. S. Yuan, and D. J. Kosman. 1998. Spectral and kinetic properties of the Fet3 protein from *Saccharomyces cerevisiae*, a multinuclear copper ferroxidase enzyme. *J. Biol. Chem.* 273:23274–23282.

17. Machonkin, T. E., H. H. Zhang, B. Hedman, K. O. Hodgson, and E. I. Solomon. 1998. Spectroscopic and magnetic studies of human ceruloplasmin: identification of a redox-inactive reduced Type 1 copper site. *Biochemistry.* 37:9570–9578.

18. Machonkin, T. E., and E. I. Solomon. 2000. The thermodynamics, kinetics, and molecular mechanism of intramolecular electron transfer in human ceruloplasmin. *J. Am. Chem. Soc.* 122:12547–12560.

19. Hellman, N. E., S. Kono, G. M. Mancini, A. J. Hoogeboom, G. J. De Jong, and J. D. Gitlin. 2002. Mechanisms of copper incorporation into human ceruloplasmin. *J. Biol. Chem.* 277:46632–46638.

20. Gitlin, J. D., J. J. Schroeder, L. M. Lee-Ambrose, and R. J. Cousins. 1992. Mechanisms of caeruloplasmin biosynthesis in normal and copper-deficient rats. *Biochem. J.* 282:835–839.

21. Gitlin, J. D. 2003. Wilson disease. *Gastroenterology.* 125:1868–1877.

22. Harris, Z. L., L. W. J. Klomp, and J. D. Gitlin. 1998. Aceruloplasminemia: an inherited neurodegenerative disease with impairment of iron homeostasis. *Am. J. Clin. Nutr.* 67 Suppl.:972S–977S.

23. De Filippis, V., V. B. Vassiliev, M. Beltramini, A. Fontana, B. Salvato, and V. S. Gaitskhoki. 1996. Evidence for the molten globule state of human apo-ceruloplasmin. *Biochim. Biophys. Acta.* 1297:119–123.

24. Sato, M., and J. D. Gitlin. 1991. Mechanisms of copper incorporation during the biosynthesis of human ceruloplasmin. *J. Biol. Chem.* 266: 5128–5134.

25. Aisen, P., and A. G. Morell. 1965. Physical and chemical studies on ceruloplasmin. 3. A stabilizing copper-copper interaction in ceruloplasmin. *J. Biol. Chem.* 240:1974–1978.

26. Vassiliev, V. B., A. M. Kachurin, M. Beltramini, G. P. Rocco, B. Salvato, and V. S. Gaitskhoki. 1997. Copper depletion/repletion of human ceruloplasmin is followed by the changes in its spectral features and functional properties. *J. Inorg. Biochem.* 65:167–174.

27. Musci, G., T. Z. Fraterrigo, L. Calabrese, and D. R. McMillin. 1999. On the lability and functional significance of the type 1 copper pool in ceruloplasmin. *J. Biol. Inorg. Chem.* 4:441–446.

28. Vachette, P., E. Dainese, V. B. Vasyliev, P. Di Muro, M. Beltramini, D. I. Svergun, V. De Filippis, and B. Salvato. 2002. A key structural role for active site type 3 copper ions in human ceruloplasmin. *J. Biol. Chem.* 277:40823–40831.

29. Sedlak, E., and P. Wittung-Stafshede. 2007. Discrete roles of copper ions in chemical unfolding of human ceruloplasmin. *Biochemistry.* 46: 9638–9644.

30. Lyubarev, A. E., and B. I. Kurganov. 1998. Modeling of irreversible thermal protein denaturation at varying temperature. I. The model involving two consecutive irreversible steps. *Biochemistry (Mosc.).* 63: 434–440.

31. Felsenfeld, G. 1960. The determination of cuprous ion in copper proteins. *Arch. Biochem. Biophys.* 87:247–251.

32. Schosinsky, K. H., H. P. Lehmann, and M. F. Beeler. 1974. Measurement of ceruloplasmin from its oxidase activity in serum by use of *o*-dianisidine dihydrochloride. *Clin. Chem.* 20:1556–1563.

33. Pina, D. G., A. V. Shnyrova, F. Gavilanes, A. Rodriguez, F. Leal, M. G. Roig, I. Y. Sakharov, G. G. Zhadan, E. Villar, and V. L. Shnyrov. 2001. Thermally induced conformational changes in horseradish peroxidase. *Eur. J. Biochem.* 268:120–126.

34. Sanchez-Ruiz, J. M., J. L. Lopez-Lacomba, M. Cortijo, and P. L. Mateo. 1988. Differential scanning calorimetry of the irreversible thermal denaturation of thermolysin. *Biochemistry.* 27:1648–1652.

35. Musci, G. 2001. Ceruloplasmin, the unique multi-copper oxidase of vertebrates. *Protein Pept. Lett.* 8:159–169.

36. Hellman, N. E., and J. D. Gitlin. 2002. Ceruloplasmin metabolism and function. *Annu. Rev. Nutr.* 22:439–458.

37. Bonaccorsi di Patti, M. C., G. Musci, A. Giartosio, S. D'Alessio, and L. Calabrese. 1990. The multidomain structure of ceruloplasmin from calorimetric and limited proteolysis studies. *J. Biol. Chem.* 265:21016–21022.

38. Plaza del Pino, I. M., B. Ibarra-Molero, and J. M. Sanchez-Ruiz. 2000. Lower kinetic limit to protein thermal stability: a proposal regarding protein stability in vivo and its relation with misfolding diseases. *Proteins.* 40:58–70.

39. Manning, M., and W. Colon. 2004. Structural basis of protein kinetic stability: resistance to sodium dodecyl sulfate suggests a central role for rigidity and a bias toward beta-sheet structure. *Biochemistry.* 43:11248–11254.

40. Baker, D., and D. A. Agard. 1994. Kinetics versus thermodynamics in protein folding. *Biochemistry.* 33:7505–7509.

41. Milardi, D., D. M. Grasso, M. P. Verbeet, G. W. Canters, and C. La Rosa. 2003. Thermodynamic analysis of the contributions of the copper ion and the disulfide bridge to azurin stability: synergism among multiple depletions. *Arch. Biochem. Biophys.* 414:121–127.

42. Pozdnyakova, I., J. Guidry, and P. Wittung-Stafshede. 2001. Copper stabilizes azurin by decreasing the unfolding rate. *Arch. Biochem. Biophys.* 390:146–148.

43. Savini, I., S. D'Alessio, A. Giartosio, L. Morpurgo, and L. Avigliano. 1990. The role of copper in the stability of ascorbate oxidase towards denaturing agents. *Eur. J. Biochem.* 190:491–495.

44. Rodriguez, J. A., J. S. Valentine, D. K. Eggers, J. A. Roe, A. Tiwari, R. H. Brown, Jr., and L. J. Hayward. 2002. Familial amyotrophic lateral sclerosis-associated mutations decrease the thermal stability of distinctly metallated species of human copper/zinc superoxide dismutase. *J. Biol. Chem.* 277:15932–15937.

45. Stockel, J., J. Safar, A. C. Wallace, F. E. Cohen, and S. B. Prusiner. 1998. Prion protein selectively binds copper(II) ions. *Biochemistry.* 37:7185–7193.

46. Sandberg, A., J. Leckner, Y. Shi, F. P. Schwarz, and B. G. Karlsson. 2002. Effects of metal ligation and oxygen on the reversibility of the thermal denaturation of *Pseudomonas aeruginosa* azurin. *Biochemistry.* 41:1060–1069.

47. Sandberg, A., D. J. Harrison, and B. G. Karlsson. 2003. Thermal denaturation of spinach plastocyanin: effect of copper site oxidation state and molecular oxygen. *Biochemistry.* 42:10301–10310.

48. Stirpe, A., L. Sportelli, and R. Guzzi. 2006. A comparative investigation of the thermal unfolding of pseudoazurin in the Cu(II)-holo and apo form. *Biopolymers.* 83:487–497.

49. Eakin, C. M., J. D. Knight, C. J. Morgan, M. A. Gelfand, and A. D. Miranker. 2002. Formation of a copper specific binding site in non-native states of beta-2-microglobulin. *Biochemistry.* 41:10646–10656.